archiDOCT

The e-journal for the dissemination of doctoral research in architecture.

Supported by the ENHSA Network | *Fueled by the* ENHSA Observatory

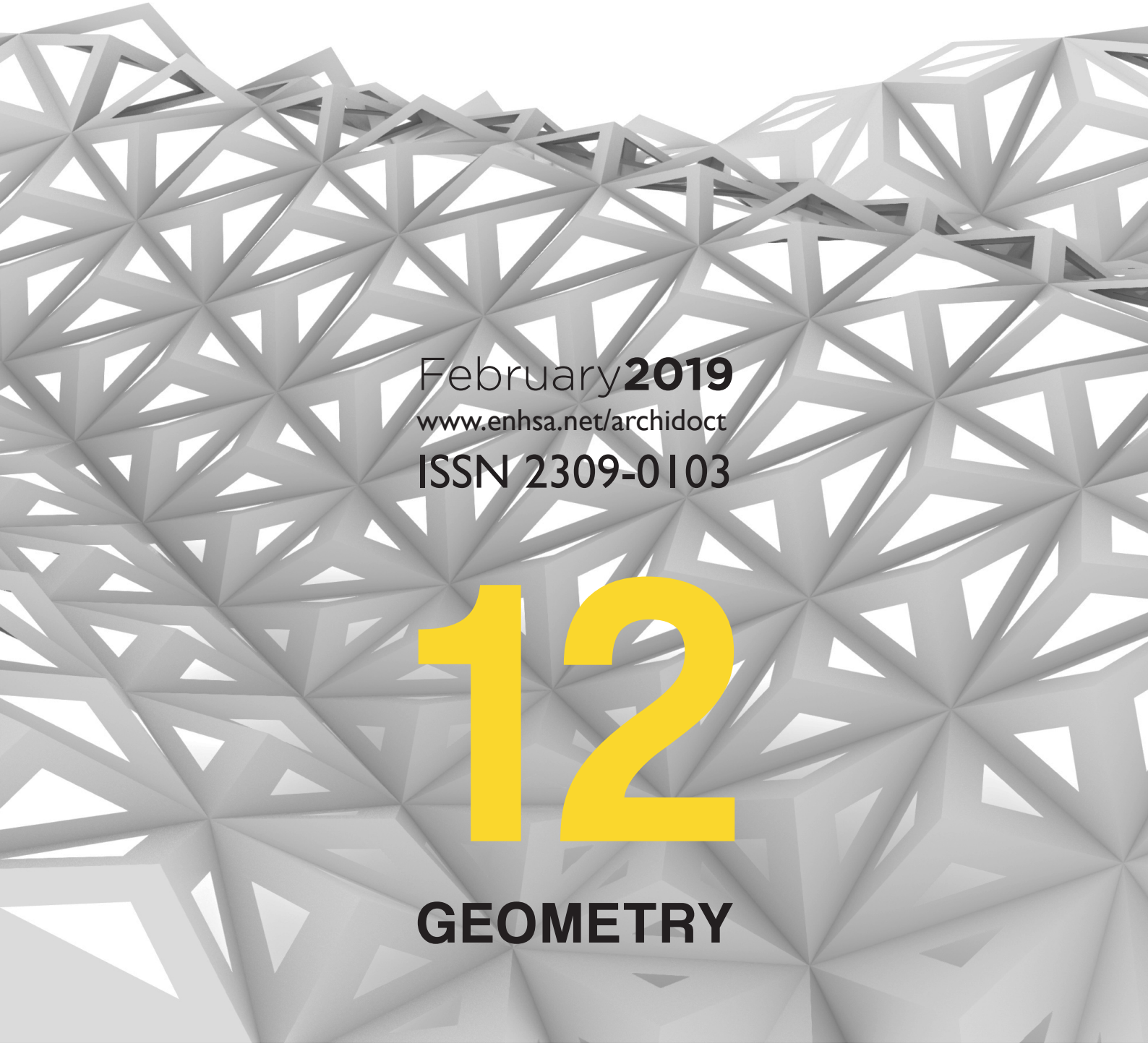

February **2019**
www.enhsa.net/archidoct
ISSN 2309-0103

12

GEOMETRY

Lifelong Learning Programme
enhsa european network of heads of schools of architecture
European Observatory of Doctoral Research in Architecture
Listed in: Scopus®

ISSN 2309-0103
www.enhsa.net/archidoct
Vol. 6 (2) / February 2019

Novel bending-active system with controllable curvature-stiffness relation

Efilena Baseta // University of Applied Arts Vienna, Austria

Abstract

This research presents a novel bending-active system, whose maximum curvature is not constrained by the required final stiffness of a given structure. This has been achieved by the development of low-tech structural elements which increase their stiffness when they reach a predefined curved geometry, relying exclusively on geometrical configurations. Physical and digital experiments have been conducted in order to document the structural performance of the latter system. More specifically, the numerical results of load-deflection experiments, as well as the Finite Element Analysis of the joinery detail are presented in this paper. The latter results prove the change of stiffness of the developed system and its scalability. The fact that the construction manual is embedded in the internal geometry of the elements, constitutes them ideal for the efficient construction of large-scale curved structures.

Keywords

Active-bending; free-form; adaptive stiffness; wood joinery; scalable systems

ISSN 2309-0103
www.enhsa.net/archidoct
Vol. 6 (2) / February 2019

1. Free-form structures

Curved elements are known for their high structural performance. Thus, they have been used to solve construction challenges through history. For instance, Romans were able to build large-span structures and revolutionized architecture by using curved architectural elements, such as arches, vaults and domes. Previous examples refer to vernacular architecture such as the easily erected temporary shelters of Arabs (Mudhif since 3300 BC), which consist of arches made of bent reeds. In addition, a pioneer Swiss engineer of the 18th century, Hans Ulrich Grubenmann, achieved to build large span timber structures, such as roofs and bridges, by using bent layered beams.

At more recent times, during 19th and 20th century, a set of simple structural typologies controlled the geometrical complexity. This was caused due to the development of reinforced concrete, as well as the industrial revolution and the need for cheap mass production (Lienhard et al. 2013). Nevertheless, in 1990s, the first digital revolution took place and affected broadly the architectural realm. A new digitally driven architectural style which illustrated the technological change of the epoch evolved; the style of spline (Carpo, 2017). At that moment, various architects proved that complex geometries can be designed and materialized by using computational software, digital fabrication techniques and materials with enhanced properties. On top of that, after the construction of the Sydney Opera (1957-73) a tendency for a 'New Structuralism' emerged. During that period, the dialogue between the architects and the engineers started to appear from the early design stages, encouraging geometrical complexity. The material started to play a very important role on the development of a structure and subsequently at the design of a form (Oxman and Oxman, 2010), likewise in vernacular architecture. Nevertheless, it was not until the second digital turn (2010s) that the construction of free-form surfaces became affordable due to technical virtuosity (Carpo, 2017).

Summarizing, it is evident that nowadays the production of curved geometries preoccupies the construction industry. However, the latter still remains expensive and labour intensive despite the fact that technology progressed. One reason is that the production of custom curved elements is time-consuming. Additionally, it requires highly qualified manufacturers and construction workers. Moreover, the need for moulds increases the construction cost and the material waste. Finally, the logistics of free-form elements are more costly compared to planar elements since they occupy larger storage and transportation space.

2. Active-bending as a construction technique for free-form geometries

In the 1960s Frei Otto initiated the construction of large-scale free-form gridshell structures (e.g. Mannheim Multihalle) out of flat beams, which were formed on-site into the desired geometry by cranes and scaffold systems (Liddell, 2015). The latter construction process was an efficient way to build curved structures since a) it eliminated the need for moulds, b) simplified the manufacturing of the elements, and c) minimized the transportation space. However, the installation was very complicated and many elements broke. As a result, in the last decade, several researchers have focused on the further development of such construction processes by implementing form-finding techniques using computational methods. Thus, active-bending, a structural system that takes advantage of the elastic deformation of specific materials in order to form curved geometries, has evolved as a new research thematic.

Many experimental pavilions have been built with the latter technique from various universities in order to optimize the design and construction processes, as well as the material performance.

ISSN 2309-0103
www.enhsa.net/archidoct
Vol. 6 (2) / February 2019

Besides that, several elastic gridshells have been built by various materials, such as aluminium tubes, glass fiber reinforced polymer (GFRP) tubes, stainless steel lamellas and bamboos (Lienhard and Gengnagel, 2018).

However, existing active-bending systems have limitations in scale (Lienhard and Knippers, 2013). The biggest the curvature that should be constructed is, the thinner the elements are, and thus the final structure is less stiff. One way to confront the latter problematic can be found in the StrechPLAY, textile-hybrid prototype. The structure is made of a laminated beam which consists of 3 GFRP rods combined into a knitted sleeve. As a result the beam is flexible during the construction (3 small cross sections) and once formed into its final configuration is impregnated with epoxy resin in order to gain its final stiffness (one larger cross section). Other researches solve the problematic by introducing additional stiffeners in the bending-active structures, such as cables and tensile fabrics (Lienhard and Knippers, 2015) (Gengnagel, Alpermann and Lafuente, 2013). Despite the good structural performance of the aforementioned structures, their construction process is complicated and time consuming.

On the contrary, the presented system suggests a novel, rapidly erected bending-active system with controllable curvature-stiffness relation, eliminating the need of extra stiffeners. This low-tech system has been achieved by leveraging geometrical configurations and material properties, like in vernacular architecture. More specifically, the system is created by multi-layered linear elements with embedded shear blocks (Fig. 1). The relative slip between the layers defines the flexibility and the final stiffness of the element. The slip is enabled by small gaps that are designed between the shear blocks of consecutive layers. The calculation of the gaps and thus the design of each element is the output of an algorithm. The input of the latter algorithm is a curve, with the predefined desired curvature, a cross section, material properties and the length of the shear blocks. The algorithm calculates the strain developed at the layers when they bend at the predefined curvature and subsequently the lengths of the required gaps (Baseta et al., 2018). The layers can be produced by digitally fabrication techniques and assembled together. The result is an element that is flexible when it is flat and stiff when it reaches its predefined curvature. The flexibility and the maximum curvature depend on the gap length. On the contrary, the final stiffness of the element depends on the number of the layers, their cross section and the frequency of the shear blocks. Thus, for the realization of an element with big curvature and high stiffness, multiple layers with small cross sectional height and big gap lengths should be made.

3. Research methodology

The methods which have been used for the development of the aforementioned bending-active system are based on physical and digital experiments. On one hand the physical experiments focus on prototypes of different materials and scales which are produced with various digital fabrication techniques. The performance of the latter prototypes is thoroughly tested and documented. On the other hand, the digital experiments rely on performance simulations and provide feedback in order to improve the physical prototypes. The evaluation of both types of experiments is vital for the optimization of the suggested construction system.

More specifically, two gridshell prototypes have been built with notched double-layered elements. The latter prototypes proved that double-layered notched linear elements, made of timber, can bend in a controlled manner. Thus, they can be self-organized into curved gridshells which consist of planar curved elements (Fig. 2) (Baseta and Bollinger, 2018). Finally, given that the discussed el-

ISSN 2309-0103
www.enhsa.net/archidoct
Vol. 6 (2) / February 2019

ements can be reverted back to their original flat configuration, and this process can be repeated several times, the system is ideal for temporary structures. The latter structures can be easily transported considering that they consist of flat elements. Moreover, they can be quickly assembled since the construction manual for each curved element is embedded in their geometry.

4. Load-deflection diagrams

In order to prove that the stiffness of the aforementioned system is controllable and independent of the curvature, physical experiments have been conducted. In the latter experiments, the deflection of cantilevering, double-layered beams with embedded shear blocked (notched) has been measured under various loads applied at the tips of the cantilevers. More specifically, three experiments have been conducted in different scales with different cross sections and lengths of the specimens (Fig. 3). The specific scales have been chosen in order to demonstrate the functionality of the system and thus its potential application in three market sectors: a) Small products, b) Furniture, and c) Architecture.

To better understand the experimental data from the tests, a basic background on the deflection of a cantilever is given here. The numerical model for the calculation of the maximum deflection of a cantilevering beam is given in the following equation:

$$u\_max=(F\ l\^3)/(3\ E\ I)$$

where umax is the maximum deflection in z direction, F the induced load, l the length of the cantilever, E the modulus of elasticity and I the moment of inertia.

Applying the above equation for solid beams to draw the corresponding load-displacement curves, a straight, inclined line is given (red curves in Fig. 6, 9 and 13). The inclination of the latter line indicates the load-deflection ratio which corresponds to the stiffness of the beam. The lines start from 0,0 since from the above equation derives that the deformation is 0 when there is no load. However, the curves that illustrate the experimental data (blue curves in Fig. 6, 9 and 13) do not start from 0,0. This is due to the deformation caused by the dead load of the specimens which is considered as the starting point of the curves.

The first experiment tests two 3D printed sticks, with a rounded zig-zag joinery detail and different gap lengths (Fig. 4). The cross section of the double layer is 5x5 mm and their length is 0.2 m. Each specimen was digitally fabricated in high quality by an Ultimaker 2 in 30 minutes. The fill was 100%, the layer height 0.2mm and the used material was Polylactic Acid (PLA). The flexibility of the latter material enables large deformations although there is a high creep rate when long term deformations are induced.

In order to collect the deformation data of the specimens, the sticks were clamped (10 mm) and 0.19 m were cantilevering. Subsequently, loads of 0.49 N, 0.98 N, 1.47 N, and 1.96 N were induced sequentially at the tip of the sticks as shown in Fig. 5b and Fig. 5c. Figure 6 shows the load-displacement graph of the aforementioned test. Both double-layered notched sticks indicate a change at the magnitude of their deflection after 1.47 N were induced (blue circle in Fig. 6). At this point, the gaps closed and thus, their cross-sectional height increased. This results in a change of the stiffness of the sticks, which is represented by the inclination of the curves. The stepper the curve is, the stiffer is

ISSN 2309-0103
www.enhsa.net/archidoct
Vol. 6 (2) / February 2019

the specimen. Moreover, the specimen c shows a slightly larger deflection than the specimen b. This is due to the longer gaps of specimen c, considering that he bigger gap of specimen c is 3 mm while the one of specimen b is 2 mm (Fig. 4).

For comparison purposes, a solid beam with cross section 5x5 mm was tested (Fig. 5a) as well as the bottom layer of beam c (Fig. 5d). From their load-displacement graphs it is evident that the specimen a is the stiffest while the specimen d is the most flexible, as expected. However, the curve of the specimen d has initially the same inclination with the specimens b and c. This verifies the fact that the double-layered notched sticks are as flexible as their layers until their embedded shear blocks are activated. Finally, the load-displacement curves of the solid sticks are not completely straight as calculated from the numerical model (red line in Fig. 6). This is possibly due to initial creep of the 3D printed stick. Nevertheless, given the small scale of the specimens and the possible imprecision of the measurements (in a scale of a millimetre) this can be neglected.

In order to receive more precise results, a second experiment with 4 times bigger cross section, made of timber has been conducted. The specimen is a robotically fabricated double-layered lath, with zig-zag joinery detail. The fabrication of the two layers lasted 15 minutes with a kuka robot. The cross section of the double layer is 20x20 mm and its length is 1.9 m (Fig. 7). The used timber is white ash, a wood which has the capacity to elastically deform with minimized creep. Moreover, the white ash was considered appropriate for the milling of small cross sections since it is dense and straight-grained. This results in a nice finishing, and thus in a more precise joinery detail.

In order to collect the deformation data of the lath, the latter was clamped in one end (0.1 m) and loads of 4.9 N, 9.8 N, 14.7 N, and 19.6 N were induced sequentially at the other end as shown in Fig. 8a. Zip ties have been placed every 0.3 m in order to keep the layers attached in y direction (perpendicular to the long axis and parallel to the ground). Figure 9a shows the load-displacement curve of the aforementioned test. The change of inclination of the curve (blue circle in Fig. 9) coincides with the moment that the shear blocks are activated, as shown in figure 8a. At that specific moment, the specimen acquires an increased stiffness with the enhanced cross section. In order to verify this behaviour, the same test has been conducted for a double-layered lath (each layer has cross section 10x20) without shear blocks (Fig. 8b). As indicated in Fig. 8, and in the corresponding load-displacement curve (b in Fig. 9), the deformation of the specimen b is larger than the one of the notched lath a. This proves that the shear blocks play an important role on the bending behaviour of the lath. Thus, double-layered linear elements with identical cross sections can bend differently according to their internal joinery details.

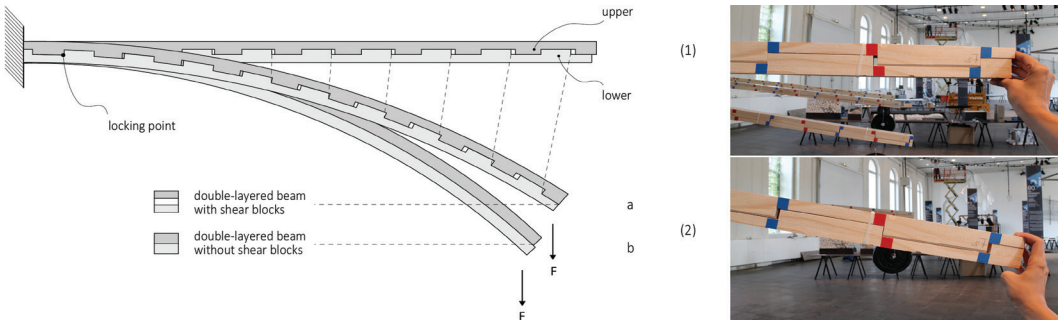

Figure 1.
Cantilevering double-layered linear element with shear blocks: 1) Flat and flexible state without forces, 2) Deformed and stiff state induced by force F (Baseta et al. 2018).

ISSN 2309-0103
www.enhsa.net/archidoct
Vol. 6 (2) / February 2019

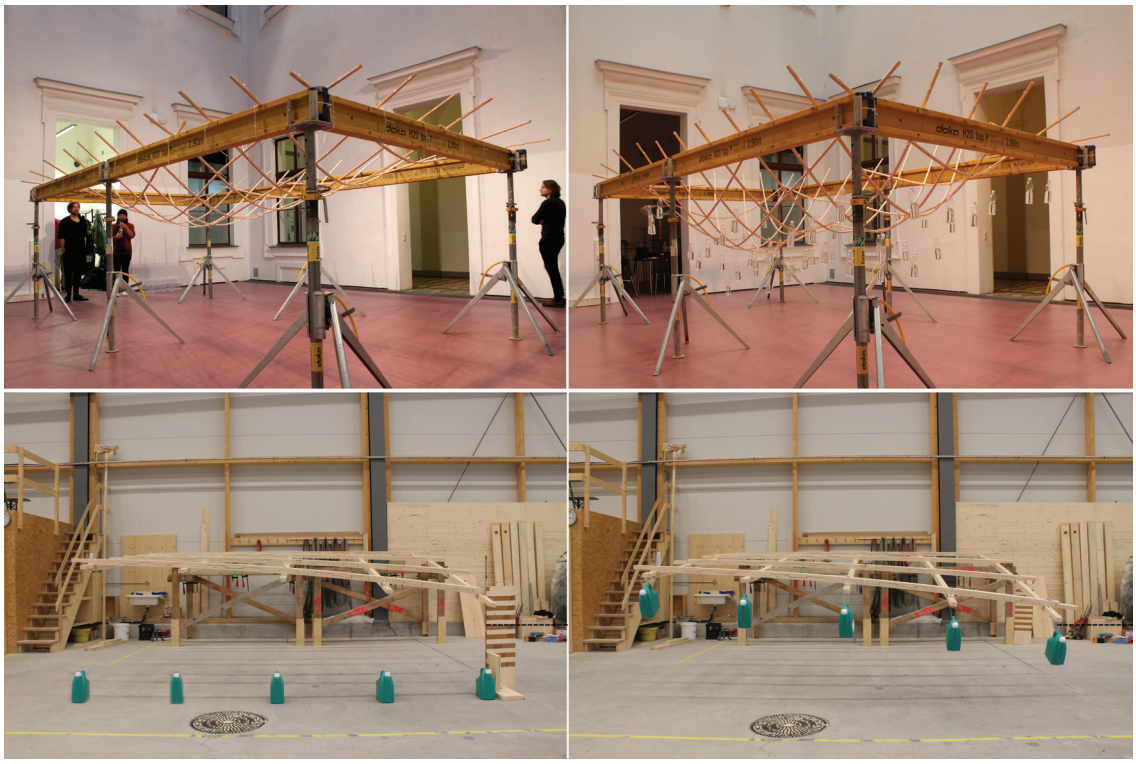

Figure 2.
Self-organized doubly-curved gridshells by gravitational loads (Baseta and Bollinger, 2018).

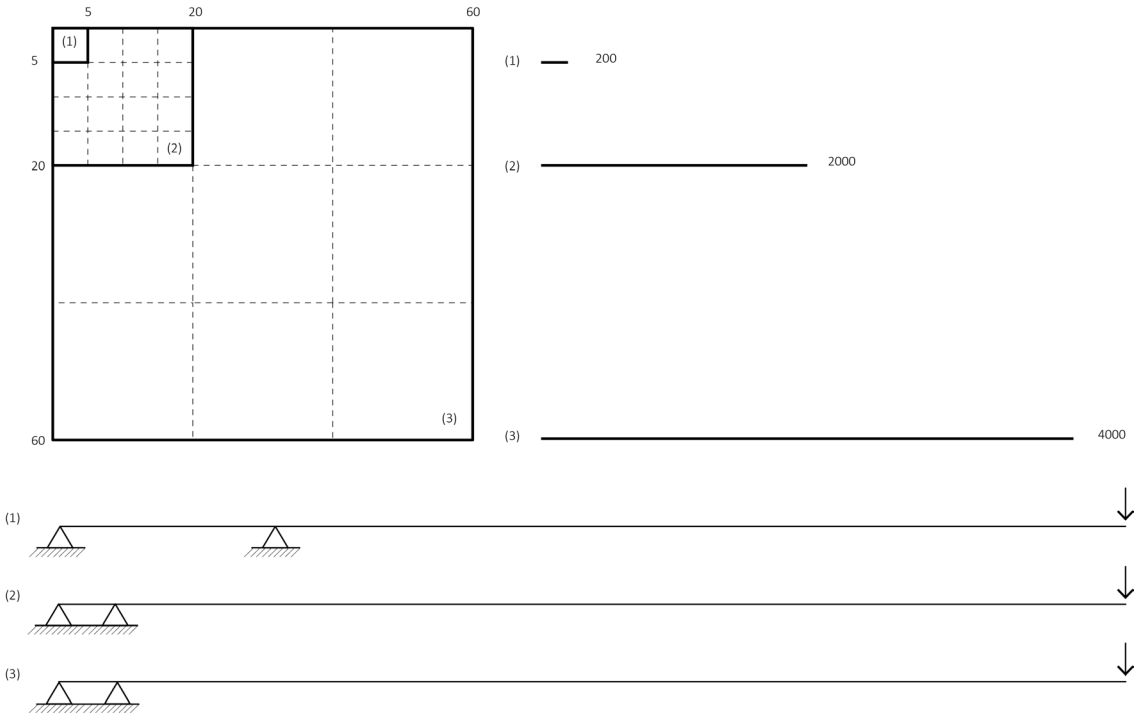

Figure 3.
Comparison of the cross sections and lengths of the specimens for the three experiments.

ISSN 2309-0103
www.enhsa.net/archidoct
Vol. 6 (2) / February 2019

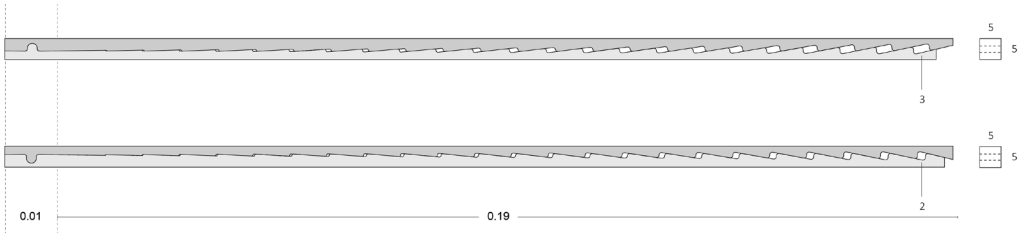

Figure 4.
Specimens for the 1st experiment (cross sections in mm and length in m).

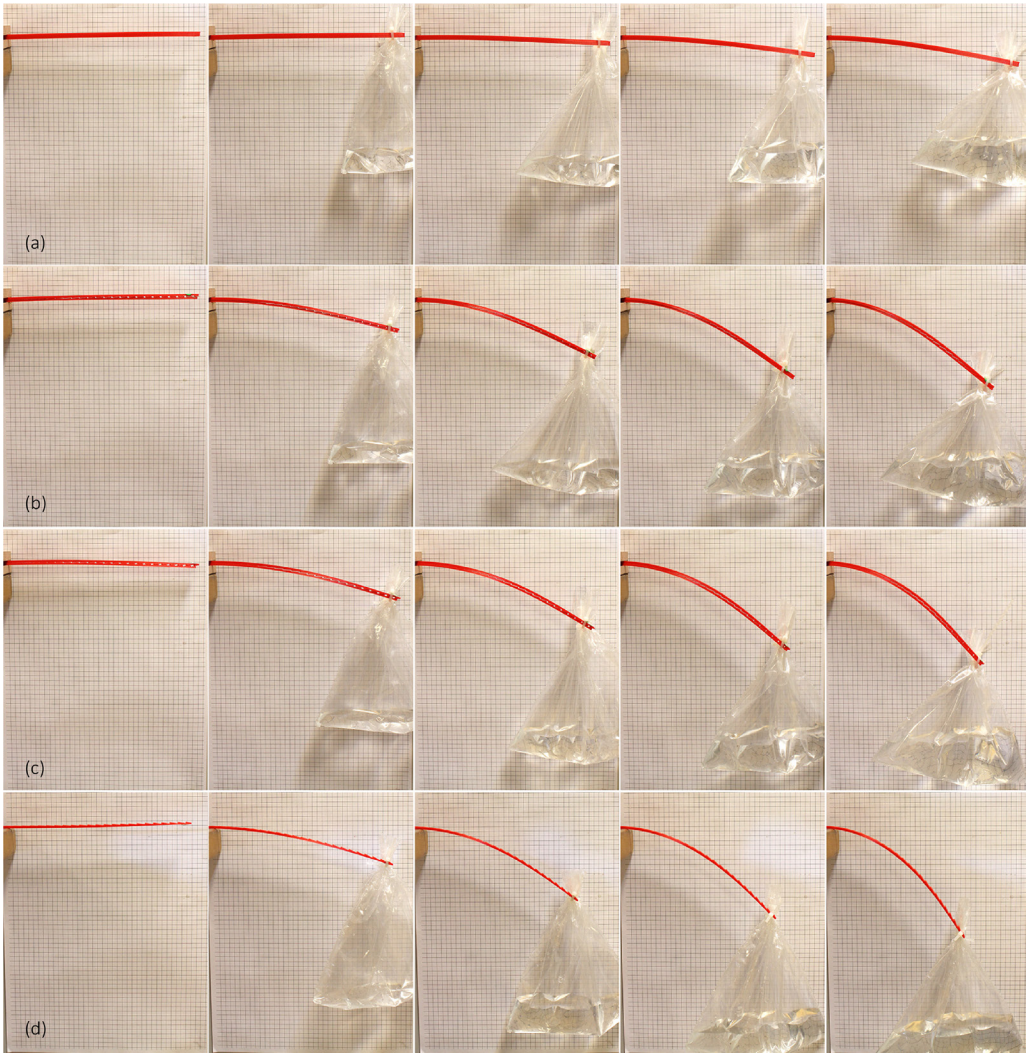

Figure 5.
Setup of the 1st experiment.

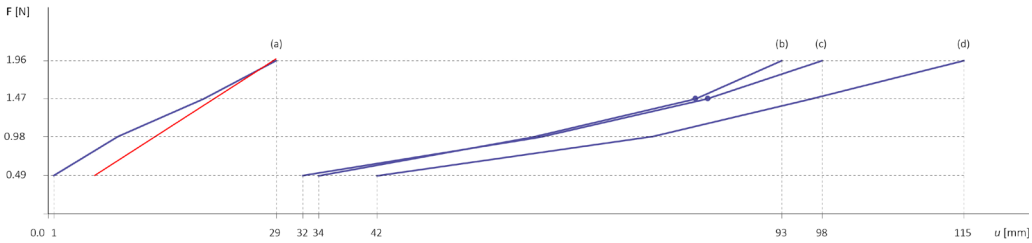

Figure 6.
Results from the 1st experiment.

ISSN 2309-0103
www.enhsa.net/archidoct
Vol. 6 (2) / February 2019

Novel bending-active system with controllable curvature-stiffness relation

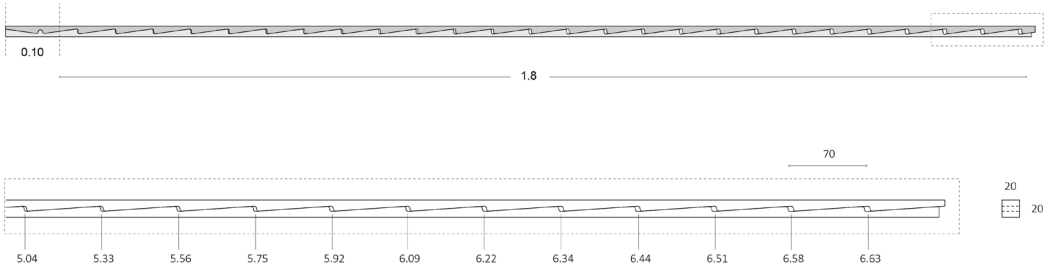

Figure 7.

Specimen for the 2nd experiment (cross sections in mm and length in m).

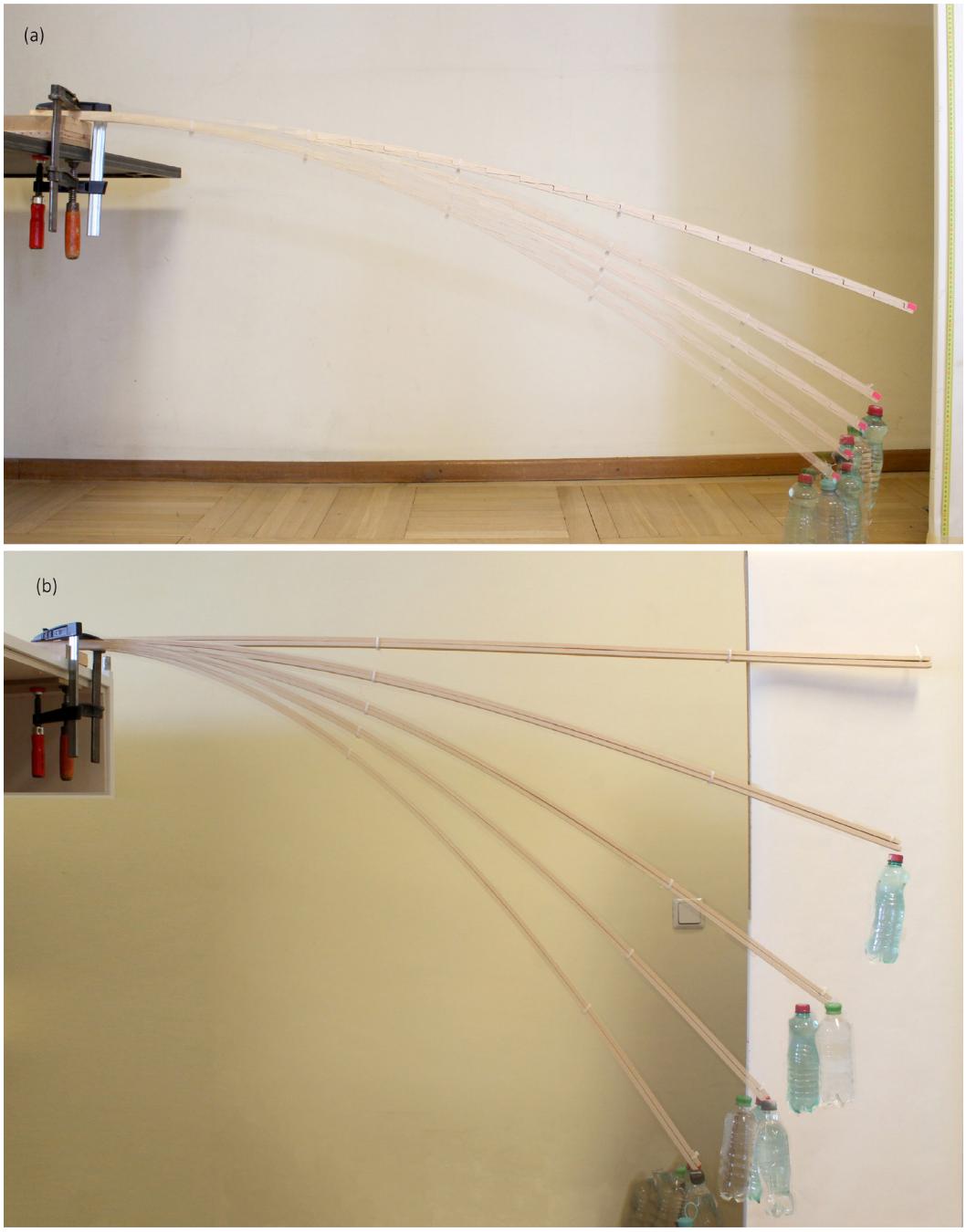

Figure 8.

Setup of the 2nd experiment: a) double-layered notched lath, b) double-layered lath without notches.

ISSN 2309-0103
www.enhsa.net/archidoct
Vol. 6 (2) / February 2019

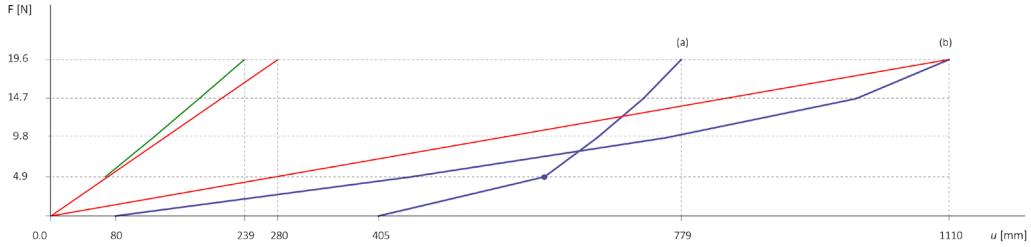

Figure 9.
Results from the 2nd experiment.

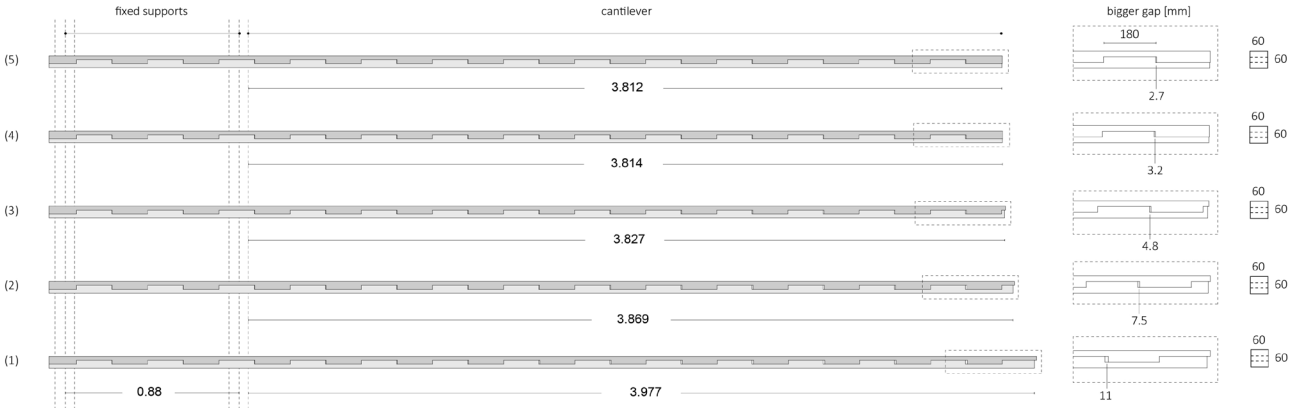

Figure 10.
Specimens for the 3rd experiment (cross sections in mm and lengths in m).

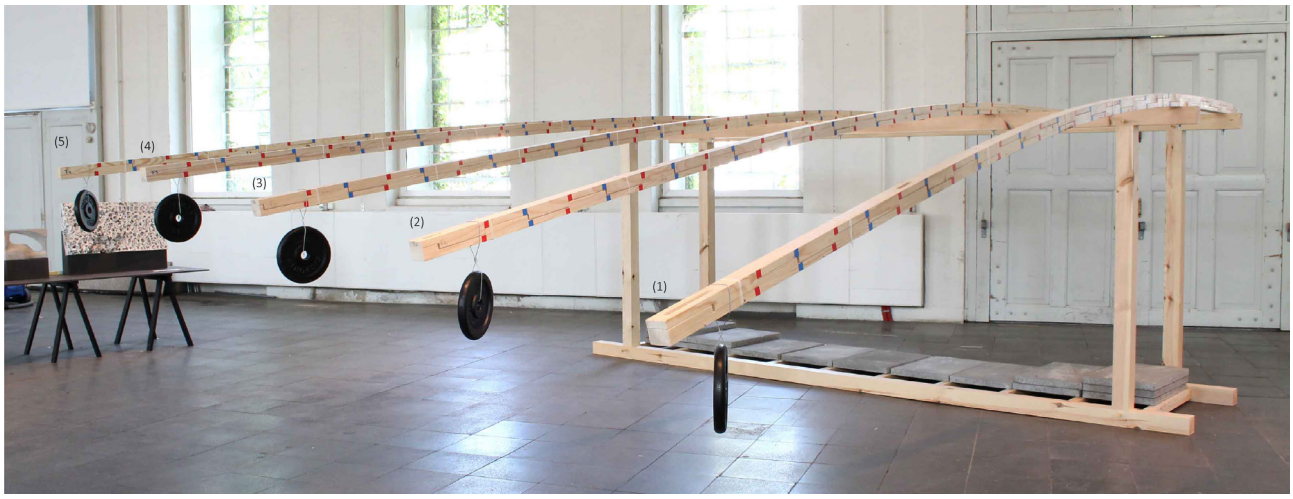

Figure 11.
Predefined deflection of beams 1-5 with 49.05 N of gravitational load.

ISSN 2309-0103
www.enhsa.net/archidoct
Vol. 6 (2) / February 2019

In order to show how the length of the internal gaps affects the bending of beams with identical cross section, a third experiment has been conducted. The specimens of this experiment have 3 times bigger cross section than the specimen of the second experiment. Due to the increase of scale, the joinery detail has been improved to a rectangular detail, parallel to the longitudinal axis of the beam. Thus, the cross-sectional height remains constant during the bending of the beam, minimizing the stresses developed at the notches. For this experiment, five beams with different gap lengths (Fig. 10) have been industrially fabricated. Their combined double cross section, fixed with zip ties every 0.6 m, is 60x60 mm and their length is approximately 5 m. The used timber is glue laminated (glulam) spruce (GL24), a low-priced, industrially fabricated glulam which is widely used in construction. The existence of very long (e.g 30 m) glulam beams made of spruce, in combination with large CNC machines like Hundegger K3, enables the rapid fabrication of large double-layered notched beams. The fabrication of each double-layered beam with the aforementioned machine lasted only 19 minutes.

Figure 11 shows the setup of the experiment. The five beams are attached to a base at two points, which span 0.88 m, with bolts (diameter 14 mm). This results to the cantilevering of approximately 4 m. The gaps of the beams 1-5 have been designed so as they bend incrementally. More specifically, beam 1 has been designed to bend at a predefined radius of curvature of 7.6 m, beam 2 at 12.07 m, beam 3 at 21.68 m, beam 4 at 41.8 m, and beam 5 at 60.6 m. The lengths of the beams slightly vary in order to achieve a uniform length in x direction (parallel to the longitudinal axis) when all the beams are bent to their predefined form (49.05 N) (Fig. 11).

In order to draw the load-deflection curve of the specimens, loads of 49.05 N, 98.1 N, 147.15 N and 196.2 N were applied sequentially at the cantilevering tip of the beams (Fig. 12a). Figure 13 shows the corresponding load-deflection curves (a in Fig. 13). As expected, the five beams deform differently under their dead load. Until they reach their predefined form (49.05 N), the beams have different stiffness. Beam 1 is more flexible and incrementally beam 5 appears to be the stiffest. After their predefined form has been reached, the stiffness of all the beams is equalized. However, the change of stiffness is more evident for beam 1 and 2, less for beam 3 and 4 and almost invisible for beam 5. Given that the longest gap of beam 5 is 2.7 mm (Fig. 10) and the fabrication tolerances are 1.5 mm it is clear that there is not a lot of room for it to act as a double-layered notched beam.

For comparison purposes, the deflection of a solid beam with equal cross section has been tested (60x60 mm GL24) (Fig. 12b). Comparing the inclination of its load-deflection curve (b and dashed blue lines in Fig.13) with the ones of the notched beams 1-5, it is evident that the stiffness of the notched beams, after they have reached their predefined curvature, is almost equal to the one of the solid beam. This proves that the gaps have closed and the beams behave as they were made from a solid, stiff cross section.

In addition to the numerical data, data from digital bending simulations have been collected for solid beams. The simulation has been done with Kangaroo2 developed by Daniel Piker and K2Eng by Cecilie Brandt (add-ons for Grasshopper 3D). A polyline divided in small segments represents a bending rod. The length of the segments of the polyline defines the bending stiffness of the 'rod' (a component of K2Eng which represents an elastic rod with bending stiffness only). Each segment of the polyline represents a 'bar', an element with only axial stiffness. The modulus of elasticity and the density of the material as well as the cross section of the beam are given as additional inputs to the definition. Moreover, 2 anchor points with high strength are placed at the fixed end of the polyline and one gravitational point load at the other end. By increasing the point load incrementally,

ISSN 2309-0103
www.enhsa.net/archidoct
Vol. 6 (2) / February 2019

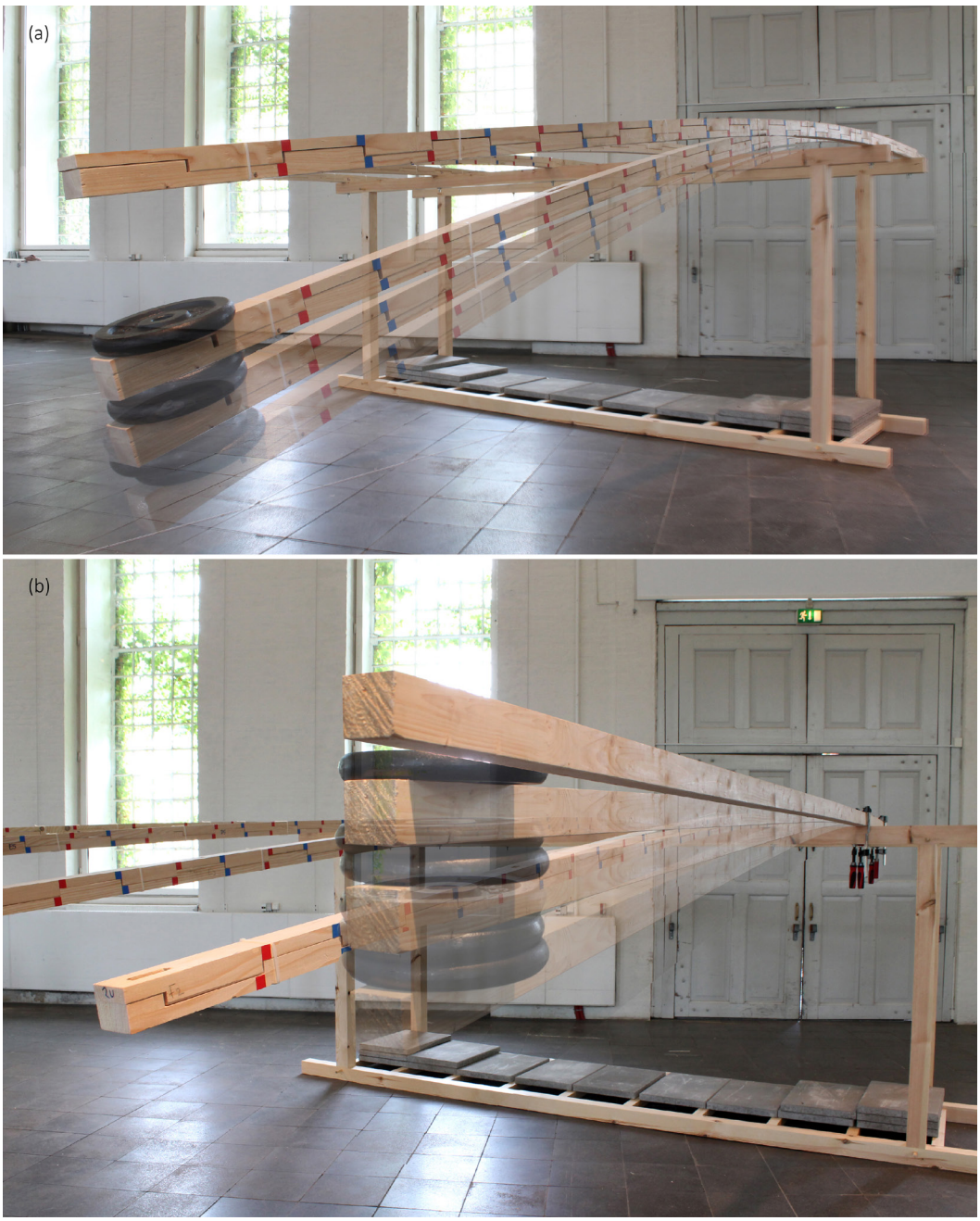

Figure 12.
Setup of the 3rd experiment: a) notched beam 1, b) solid beam.

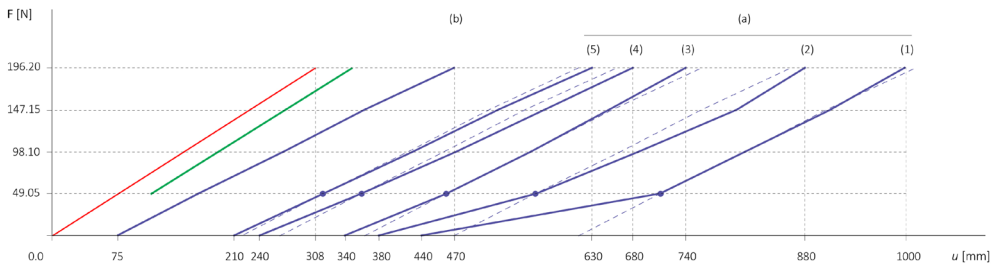

Figure 13.
Results from the 3rd experiment.

ISSN 2309-0103
www.enhsa.net/archidoct
Vol. 6 (2) / February 2019

mimicking the loading of the physical tests, the maximum deflection (in z direction) of the polyline is the output of the Kangaroo2 solver (Fig. 14). Apart from the aforementioned data, the solver can output the axial and the shear forces, the bending stresses and moments, as well as the reactions of the supports.

By using the digital simulations, visual understanding of the bending behaviour of various scales and materials can be achieved, reducing the need for physical tests. The load-deflection curve of the solid beam 60x60 mm (green in Fig. 13) has been created from the data extracted from the aforementioned simulation. The fact that the latter curve lies between the curve from the numerical (red in Fig. 13) and the experimental (b blue in Fig. 13) data indicates that the developed digital simulation is a reliable mean to predict the bending behaviour of a solid beam. This is an important step towards the development of a simulation for the double layered notched beams.

In conclusion, similar bending behaviour of the double-layered elements with the shear blocks is observed in the three different scales. This verifies that the developed system is scalable. The desired use of the system and the maximum stresses that it should resist define the material. Materials with high strength and deformability are the most appropriate for active bending systems. Some of the latter materials are wood, bamboo, Glass Fibre Reinforced Polymers (GFRP), Natural Fibre Reinforced Polymers (NFRP) and aluminium (Kotelnikova-Weiler et al., 2013). 3D printing of synthetic composites and CNC milling of natural solid materials are two of the main digital fabrication techniques which can be used to produce the discussed elements.

5. Finite Element Analysis of the joinery detail

As mentioned above, the design of the joinery detail is the most crucial parameter in order to achieve the maximum stiffness and avoid breakages of the discussed system. The zig-zag detail has the disadvantage that during bending the cross-sectional height of the double layered notched element decreases, as the one layer slides into the other in an inclined manner. This fact could be problematic for some applications. Therefore, variations of the rectangular detail have been explored further with Finite Element Method (FEM).

More specifically, Karamba3D developed by Clemens Preisinger (add-on of Grasshopper3D) has been used for the structural analysis of the detail. A small segment of a double-layered beam has been selected to be analysed. The simplified digital structural model consists of two two-dimensional meshes which represent the two layers as 'shells'. The mesh is more refined only close to the contact points of the two layers in order to get more detailed values in the areas of interest and make the analysis faster. The two shells are independent and connect only through lines defined as 'trusses' (elements with axial and no bending stiffness) with small cross section. The trusses are placed perpendicular to the contact edges of the two shells. Thus, along the contact edge, only axial forces, such as compression can be developed. The bottom shell is fixed with supports at its bottom edge and the top shell slides towards the bottom with 'prescribed displacements' at its supports at the top edge. (Fig. 15)

The Finite Element Analysis (FEA) of Karamba3D outputs the displacement of the shells as well as their utilization, principal and Van Mieses stresses. Three different angles of the contact edge have been analysed, 0o (perpendicular to the long axis), - 45 o and 45 o. In Figure 15 the colours represent the principal stresses induced when the two shells are forced to contact. The red represents

ISSN 2309-0103
www.enhsa.net/archidoct
Vol. 6 (2) / February 2019

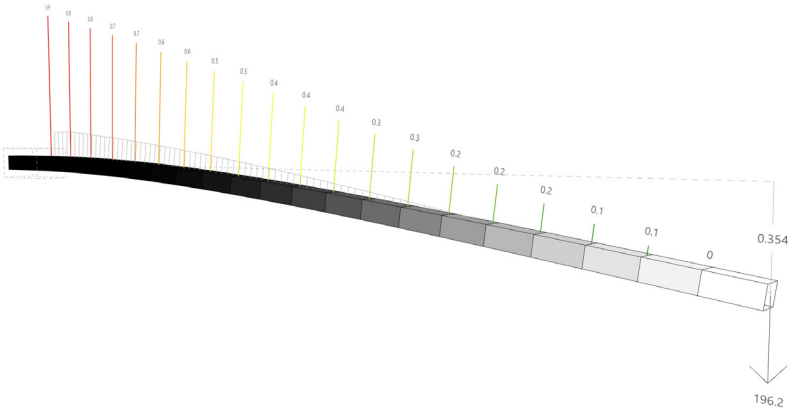

Figure 14.
Maximum deflection of the solid beam from the 3rd experiment extracted from digital experiment. The moments, for each segment of the original polyline, appear with different colours.

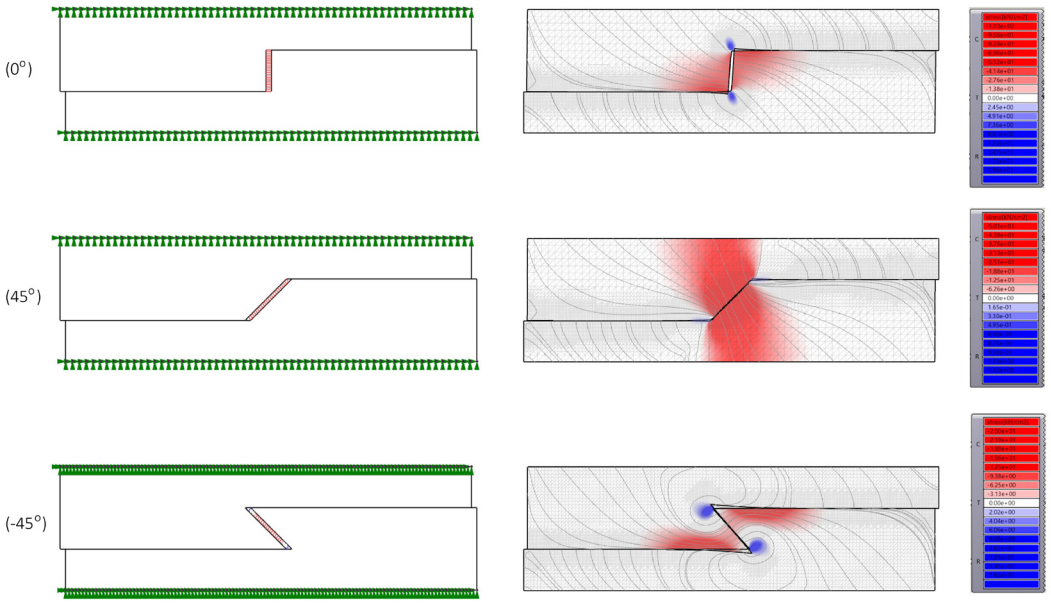

Figure 15.
Setup and results from the FEA of 3 different joinery details.

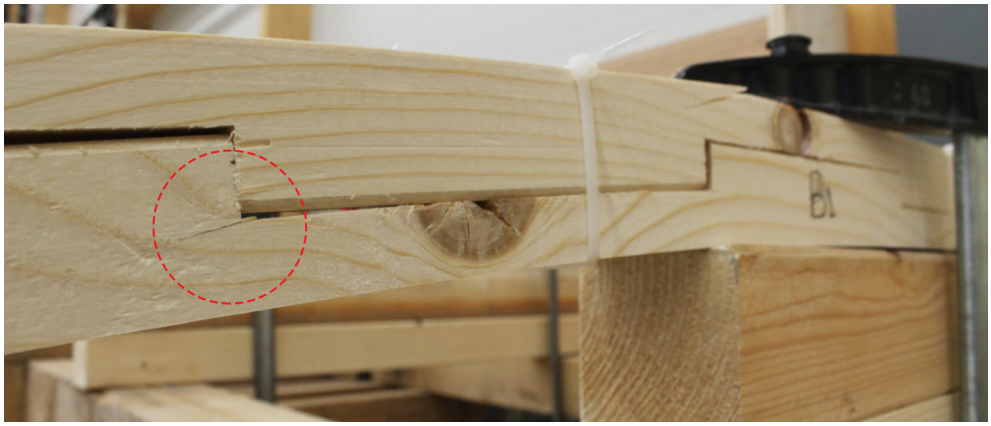

Figure 15.
Setup and results from the FEA of 3 different joinery details.

ISSN 2309-0103
www.enhsa.net/archidoct
Vol. 6 (2) / February 2019

the compressive stresses and the blue the tensile stresses. From this FEA it is evident that the problematic areas are the blue areas at the ends of the contact edges, which is verified by a physical strength test (Fig. 16). Looking at the values of the stresses, the bigger areas with tensile stresses are developed at the - 45 o angle specimen. As a result, this joinery detail is more susceptible to breakages. On the contrary, the 45 o angle specimen shows the smaller tensile stresses and the maximum compressive stresses, which makes the specimen the optimal shear block in comparison with the other two specimens.

6. Conclusion

This paper proposed an alternative way to produce curved structural elements, with both big curvature and high stiffness, in various scales. The developed system relies on multi-layered elements which can be formed easily into a predefined geometry when they bend. The discussed research focuses on 1D linear elements which can form planar curves. However, there is potential to extend it to 2D elements. The method to prove the structural performance of the developed system was the physical experiment. In the conducted experiments, the deflection of the discussed elements was measured under various loads. The extracted experimental data proved that the elements increase their stiffness when they reach their predefined form, relying exclusively on geometrical configurations and material properties. Thus, curved elements can be easily produced with digital fabrication techniques and rapidly construct free-form geometries, considering that their construction manual is embedded in their joinery details. The optimization of the latter details can improve the performance of the elements, therefore FEA has been employed. Future goal of the research is to develop a digital simulation of the kinetic and structural behaviour of the proposed elements, so as the designer can predict their performance, eliminating the need for physical prototypes. Finally, case studies for the application of the system in three different scales (small products, furniture, and architecture) are yet to be developed.

Acknowledgments

This project has received funding from the European Union's Horizon 2020 research and innovation program under the Marie Sklodowska-Curie grant agreement No 642877.
The fabrication of the large-scale timber beams would not have been possible without the support from the Blumer Lehmann AG (Gossau, Switzerland) team and its leaders Kai Strehlke and Martin Antemann.

The robotic fabrication of the small scale timber lath would not have been possible without the support from Philipp Hornung from the Angewandte Robotic Lab and the Wood technology laboratory of the University of Applied Arts Vienna.

ISSN 2309-0103
www.enhsa.net/archidoct
Vol. 6 (2) / February 2019

References

Alquist, S., 2015. Social Sensory Architectures: Articulating Textile Hybrid Structures for Multi-Sensory Responsiveness and Collaborative Play. In: *Computational Ecologies: Design in the Anthropocene - ACADIA 2015,* Cincinnati: University of Cincinnati, pp. 262-271.

Baseta, E. and Bollinger, K., 2018. Construction system for reversible self-formation of gridshells: Correspondence between physical and digital form. In: *Recalibration on imprecision and infidelity - ACADIA 2018*. Mexico City: Universidad Iberoamericana, pp. 366-375.

Baseta, E., Preisinger, C., Antemann, M., Strehlke, K. and Bollinger, K., 2018. Geometry-induced variable stiffness structures. In: *IASS Symposium 2018 - Creativity in Structural Design*. Boston: Massachusetts Institute of Technology.

Carpo, M., 2017. *The second digital turn – Design beyond intelligence*. Cambridge, MA: The MIT Press, p.55-65.

Gengnagel, C., Alpermann, H. and Lafuente, E., 2013. Active Bending in Hybrid Structures. In: H. Günther, R. Maleczek and C. Scheiber,ed., *FORM – RULE | RULE – FORM 2013*. Innsbruck: Innsbruck University Press.

Kotelnikova-Weiler, N., Douthe, C., Lafuente, E., Baverel, O., Gengnagel, C. and Caron, J., 2013. Materials for Actively-Bent Structures. *International Journal of Space Structures*, 28 (3-4), pp. 229-240.

Liddell, I., 2015. Frei Otto and the development of gridshells. *Case Studies in Structural Engineering*, 4, pp. 39–49.

Lienhard, J., Alpermann, H., Gengnagel, C. and Knippers, J., 2013. Active Bending, a Review on structures where bending is used as a self-formation process. *International Journal of Space Structures*, 28(3-4), pp. 187-196.

Lienhard, J. and Gengnagel, C., 2018. Recent development in bending-active structures. In: *IASS Symposium 2018 - Creativity in Structural Design*. Boston: Massachusetts Institute of Technology.

Lienhard, J. and Knippers, J., 2015. Bending-Active Textile Hybrids. J*ournal of the International Association for Shell and Spatial Structures*, 56, pp. 37-48.

Lienhard, J. and Knippers, J., 2013. Considerations on the Scaling of Bending-Active Structures. *International Journal of Space Structures* 28 (3-4), pp. 137–148.

Oxman, R. and Oxman, R., 2010. *The new structuralism design, engineering and architectural technologies.* London: AD Wiley Academy, pp. 15.